Langmuir

Article

pubs.acs.org/Langmuir

Centimeter-Scale Subwavelength Photolithography Using Metal-Coated Elastomeric Photomasks with Modulated Light Intensity at the Oblique Sidewalls

Jin Wu,[‡] Yayuan Liu,[‡] Yuanyuan Guo,[‡] Shuanglong Feng,[‡] Binghua Zou,[†,‡] Hui Mao,[‡] Cheng-han Yu,[§] Danbi Tian,[∥] Wei Huang,[†] and Fengwei Huo*[,†,‡]

[†]Key laboratory of Flexible Electronic (KLOFE) & Institute of Advanced Materials (IAM), Jiangsu National Synergistic Innovation Center for Advanced Materials (SICAM), Nanjing Tech University, 30 South Puzhu Road, Nanjing 211816, People's Republic of China

[‡]School of Materials Science and Engineering, Nanyang Technological University, 50 Nanyang Avenue Singapore 639798, Singapore

[§]Department of Anatomy, Li Ka Shing Faculty of Medicine, University of Hong Kong, Hong Kong, People's Republic of China

[∥]College of Science, Nanjing Tech University, Puzhu Road, Nanjing 211816, People's Republic of China

Supporting Information

ABSTRACT: By coating polydimethylsiloxane (PDMS) relief structures with a layer of opaque metal such as gold, the incident light is strictly allowed to pass through the nanoscopic apertures at the sidewalls of PDMS reliefs to expose underlying photoresist at nanoscale regions, thus producing subwavelength nanopatterns covering centimeter-scale areas. It was found that the sidewalls were a little oblique, which was the key to form the nanoscale apertures. Two-sided and one-sided subwavelength apertures can be constructed by employing vertical and oblique metal evaporation directions, respectively. Consequently, two-line and one-line subwavelength nanopatterns with programmable feature shapes, sizes, and periodicities could be produced using the obtained photomasks. The smallest aperture size and line width of 80 nm were achieved. In contrast to the generation of raised positive photoresist nanopatterns in phase shifting photolithography, the recessed positive photoresist nanopatterns produced in this study provide a convenient route to transfer the resist nanopatterns to metal nanopatterns. This nanolithography methodology possesses the distinctive advantages of simplicity, low cost, high throughput, and nanoscale feature size and shape controllability, making it a potent nanofabrication technique to enable functional nanostructures for various potential applications.

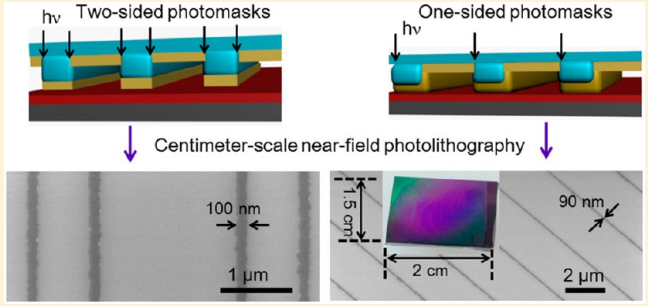

INTRODUCTION

Lithography is of great demand in fabrication of integrated circuits (ICs), microelectromechanical systems (MEMS), chemical and biological sensors, microfluidics, and subwavelength optical components.[1−9] Particularly, nanopatterns are also of great importance in studying cell−matrix interaction in recent years.[10−14] The fabrication of nanoscale features over large areas in a low-cost manner is a significant objective in nanotechnology community for both industrial and academic applications.[8,15−25] However, some important factors such as low cost, high productivity, and controllable feature size (especially for subwavelength size) are often in conflict with each other for current lithographic strategies,[8,26] such as conventional far-field photolithography, electron beam lithography (EBL),[27] and the serial scanning probe based lithography (SPL).[28,29] Block copolymer lithography[30,31] and interference lithography[32] can produce high-resolution regular nanopatterns over large areas, while arbitrarily shaped nanopatterns are prohibited by these methods. Molecular lithography[21,33] and soft lithography[20] based on transferring self-assembled monolayers (SAMs) from tips to surfaces aroused broad interest and realized extensive applications. Nevertheless, these methodologies require selective wet etching to fabricate metal nanostructures, which induces metal residuals on substrates and the difficulty in controlling the etching time.[20,21,33] Until now, photolithography remains the major workhorse for massive production of micro/nanoscale devices owning to its merits of highly parallel process, well-established procedures, and highly reproducible results.[1,8,26,34] However, the resolution of conventional photolithography is restricted by far-field light diffraction limit.[8,9] Near-field photolithography is a promising strategy to enable subwavelength nanopatterns by circumventing the far-

Received: February 12, 2015
Revised: April 9, 2015
Published: April 13, 2015

DOI: 10.1021/acs.langmuir.5b00568
Langmuir 2015, 31, 5005−5013

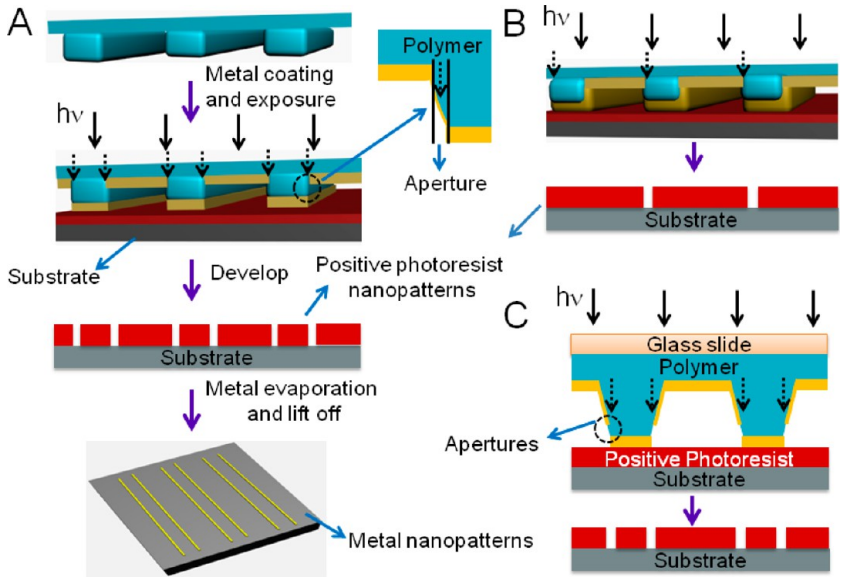

Figure 1. Schematic illustrating subwavelength near-field photolithography using metal-coated elastomeric photomasks to modulate the transmission light intensity at the sidewalls. (A) Light leaks from two-sided apertures created at the sidewalls of PDMS reliefs to produce two-line subwavelength nanopatterns. (B) Light leaks from one-sided apertures constructed at the sidewalls to produce one-line subwavelength nanopatterns. (C) Light leaks from the nanoscopic apertures created at the oblique sidewalls of PDMS reliefs to expose underlying photoresist, producing subwavelength nanopatterns. The size adjustable oblique sidewalls were obtained from anisotropic etching of silicon.

field diffraction limit.[3,17,35−42] For example, a massive desktop nanofabrication strategy termed beam pen lithography (BPL) has been developed to enable subwavelength nanopatterns by utilizing a metal-coated polydimethylsiloxane (PDMS) tip array with nanoscopic apertures created at the apexes of tips for near-field photolithography.[8,9,41] However, the difficulty in construction of uniform nanoscopic apertures at the apexes of a large-area tip array as well as the demand of expensive SPL platform restricts the practical application of BPL.

A cost-effective phase shifting photolithography (PSP) was developed to fabricate sub-100 nm nanostructures by employing the phase shift effect introduced by transparent PDMS reliefs at the edges.[17,22,43−45] The PDMS reliefs with proper relief depth can shift the transmitted light by odd numbers of π radians, leading to nearly null intensity at the edges of PDMS reliefs.[43,45] However, all the photoresist except that below the sidewalls of PDMS reliefs is exposed due to the transparent nature of PDMS reliefs, which makes the produced raised positive photoresist nanopatterns unfavorable to be transferred to other materials. In principle, it is desirable to allow underlying photoresist to be exposed only at nanoscale areas, such as the areas below the edges of PDMS reliefs. We hypothesize that coating PDMS relief structures with a layer of opaque metal such as gold could be an effective means to achieve this aim. Theoretically, it is impossible because the opaque metal layer may block all the transmission of incident light through the PDMS reliefs if these PDMS reliefs have absolutely vertical sidewalls. However, we find that PDMS micro/nanostructures replicated from the rigid silicon molds cannot have absolutely vertical sidewalls due to the elastic property of this polymer.[46,47] There is a narrow transitional region at each sidewall, where the corners are round in nanoscale dimension (Figure 1A,B). The metal layer at the oblique sidewalls is thinner than that at other regions because of the line-of-sight characteristic of electron-beam evaporation and larger surface areas at the sidewalls as compared with other regions in the vertical direction, leading to the formation of nanoscale apertures at the sidewalls. Therefore, light can be exclusively allowed to pass from the nanoscopic apertures to expose underlying photoresist at nanoscale areas, which enables the production of subwavelength nanopatterns. Importantly, it is assumed that the absolutely vertical sidewalls of PDMS reliefs are responsible for phase shift effect in PSP previously.[16,22,43,45] However, herein we find that the sidewalls of elastomeric PDMS reliefs are slight slopes, which may play the key roles in both PSP and the subwavelength photolithographic strategy developed in this study.

Noticeably, the nanoscopic apertures can be created in one step manner at the sidewalls of PDMS reliefs during the metal coating process, bypassing the requirement of extra and complicated procedures after metal coating as in the cases of BPL and other apertures-based near-field photolithography strategies.[8,9,37,39] Particularly, the apertures could be created on either both sides (Figure 1A) or one side (Figure 1B) of each PDMS relief stripe using vertical or oblique metal evaporation direction, respectively. Consequently, two-line (Figure 1A) and one-line (Figure 1B) nanopatterns with various shapes could be produced by utilizing the obtained light leaking photomasks. Besides, the light leaking photomasks with intentionally designed oblique sidewalls could also be used to generate subwavelength nanostructures by utilizing the light leaking from nanoscale apertures or thin opaque metal coated oblique sidewalls of PDMS reliefs (Figure 1C). Additionally, photoresist nanopatterns with various shapes could be transferred to subwavelength metal nanostructures over square centimeter areas with fidelity using the lift-off method.

EXPERIMENTAL SECTION

Fabrication of the Silicon Masters of PDMS Reliefs. The Si/SiO_2 (100) wafers with the SiO_2 layer thicknesses of 2 μm, 600 nm, and 260 nm were spin-coated with Shipley1805 (MicroChem) photoresist to perform conventional far-field photolithography on the mask aligner (SUSS MJB4 UV400 from SUSS MicroTec Co.). Conventional chromium photomasks with micrometer-sized patterns

DOI: 10.1021/acs.langmuir.5b00568
Langmuir 2015, 31, 5005−5013

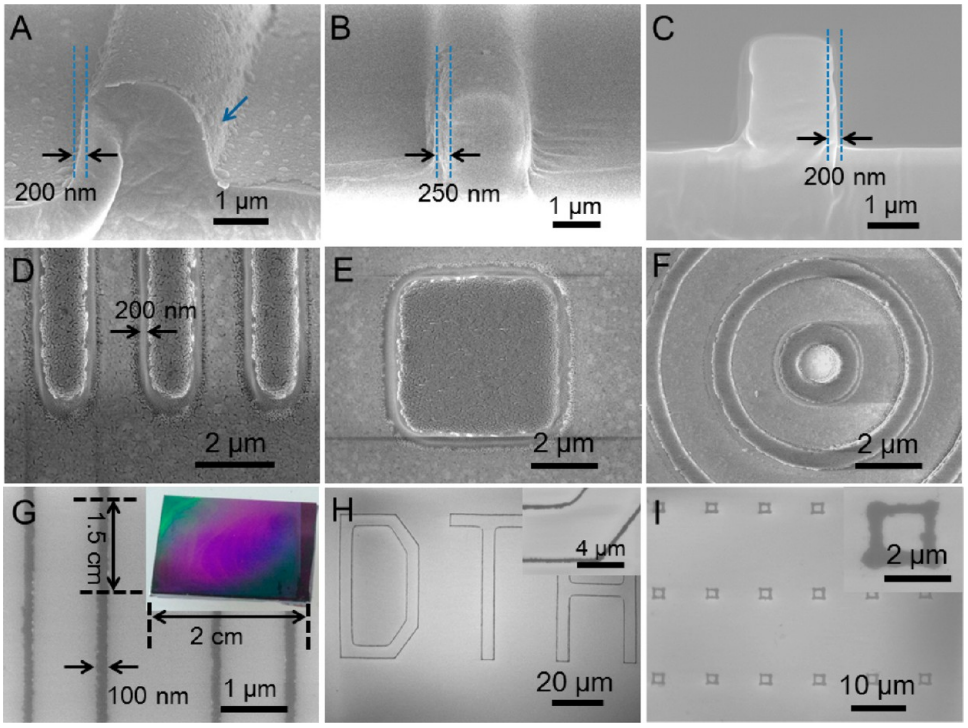

Figure 2. Subwavelength photolithography with the elastomeric photomasks with two-sided apertures. (A) SEM cross-sectional image of 60 nm gold-coated PDMS reliefs demonstrated that the gold layer at the oblique sidewalls was thinner than that at other regions. (B) SEM cross-sectional image of soft PDMS reliefs without metal coating demonstrated that the oblique sidewalls had the slope size of 250 nm. (C) SEM cross-sectional image of the hard PDMS reliefs without metal coating demonstrated that the oblique sidewalls had the slope size of 200 nm. (D, E, F) SEM top-down images of 200 nm wide two-sided apertures created at the sidewalls of PDMS reliefs with the shapes of straight line, square, and multiple-circle, respectively. (G, H, I) SEM images of Cr nanopatterns with the shapes of straight lines, miniaturized letters of "DTH" and square, respectively. Inset of (G) was optical image of 100 nm wide positive photoresist nanopatterns fabricated on SiO_2/Si substrate over the areas of 2 × 1.5 cm^2.

of different shapes were used, such as rectangular, square, circular, branch, ellipse, ladder, and miniaturized letters. After exposure, the photoresist was developed in MF319 (MicroChem). For fabricating the silicon masters with vertical sidewalls, the obtained samples were subjected to etching in a commercially buffered hydrofluoric acid (Transene Co.) for several minutes until the unprotected SiO_2 was completely removed and the silicon surfaces in the features were exposed. The required etching time was different for the SiO_2 layers with different thickness. Subsequently, the photoresist on sample surfaces was removed by rinsing in acetone. For fabrication of the silicon masters with oblique sidewalls, the above HF-treated samples were placed in the KOH etching solution (30% KOH in H_2O:isopropanol (4:1 v/v)) at 75 °C with vigorous stirring to etch the exposed silicon anisotropically, leading to the formation of recessed silicon trench array. Since the apexes size of silicon trenches decreased with the prolonged etching time, the apexes size of silicon masters could be adjusted by controlling the etching time (Figure S9 in Supporting Information). The remaining SiO_2 was removed by immersing the substrates in buffered hydrofluoric acid for sufficient time (6 min). Finally, 1*H*,1*H*,2*H*,2*H*-perfluorodecyltrichlorosilane (Gelest) was used to modify the silicon masters by gas-phase silanization in order to facilitate the release of PDMS reliefs from the silicon molds.

Fabrication of PDMS Light Leaking Photomasks. Hard PDMS (h-PDMS) was composed of 3.4 g of vinyl-compound-rich prepolymer (VDT-731, Gelest) and 1.0 g of hydrosilane-rich cross-linker (HMS-301). 20 ppm w/w platinum catalyst (platinum divinyltetramethyldisiloxane complex in xylene, SIP 6831.1, Gelest) and 0.1% w/w modulator (2,4,6,8-tetramethyltetravinylcyclotetrasiloxane, Fluka) were added into the vinyl fraction. The mixture was stirred, degassed, and poured on top of the above fabricated silicon molds. For preparing the elastomeric light leaking photomasks with rigid glass support, a precleaned and oxygen plasma treated hydrophilic glass slide (VWR, Inc.) was then placed on top of the elastomer array. After the whole assembly was cured at 70 °C overnight, the glass slide supported PDMS structures were carefully separated from the silicon masters. For preparing elastomeric light leaking photomasks without rigid glass covers, the above-mentioned mixture was poured on the silicon masters with the PDMS layer thickness around 4 mm without covering glass slide before curing the whole assembly. The obtained PDMS relief structures were coated with 60 nm thick gold by using electron-beam evaporation to make them opaque. For fabrication of the light leaking photomasks with two-sided apertures, the PDMS reliefs were placed vertically above the metal source during metal evaporation process. For preparation of the light leaking photomasks with one-sided apertures, the samples were placed away from the metal source in the vertical direction during the evaporation of metal, such as right above or left above the metal source.

Lithography on Positive-Tone Photoresist Surface. The Shipley1805 (MicroChem) photoresist was prediluted with propylene glycol monomethyl ether acetate (MicroChem). The diluted photoresist was spin-coated on Si/SiO_2 (100) wafers at 3000 rpm for 30 s. The 30% (v/v) and 20% (v/v) diluted photoresist was used to obtain a 70 nm thick and 40 nm thick photoresist layer, respectively. The resulting photoresist-coated substrates were baked on hot plate at 110 °C for 5 min before being used for near-field photolithography. The light leaking photomasks were placed directly on the photoresist coated surfaces manually for photolithography. Thanks to the elastomeric characteristic of PDMS, the PDMS reliefs with nanoscopic apertures could contact intimately with underlying photoresist surface. A halogen light source (Fiber-lite Illuminators MI150, Dolan-Jenner) with adjustable power from 0 to 250 mW/cm^2 was used to expose the photoresist. The typical exposure time for a 400 nm halogen lamp with the exposure energy of 200 mW/cm^2 was 2 s, followed by the photoresist development in MF319 (MicroChem) for 40 s. Typically, 10 nm Cr or 5 nm Cr/10 nm Au was evaporated on the developed

DOI: 10.1021/acs.langmuir.5b00568
Langmuir 2015, 31, 5005−5013

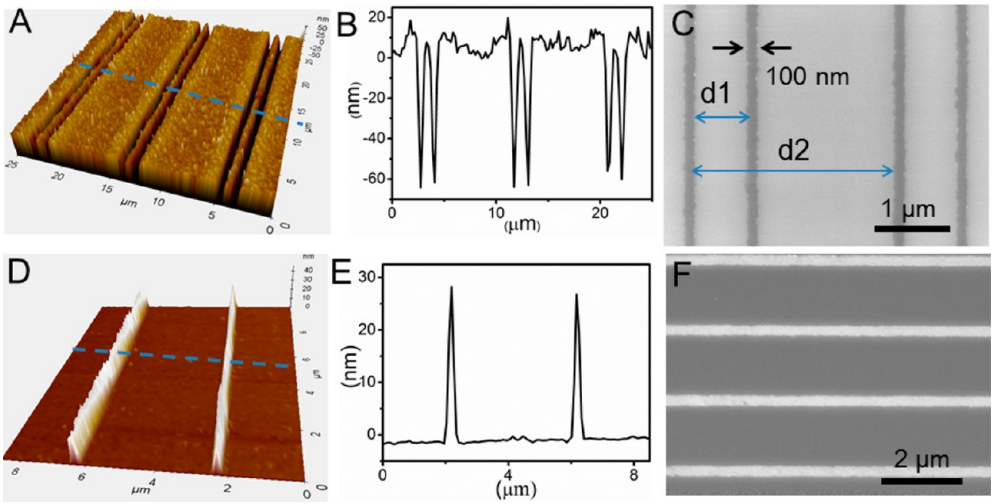

Figure 3. Comparison between the nanopatterns produced in this lithographic strategy (A–C) and that in PSP (D–F). (A) Three-dimensional atomic force microscopy (AFM) topographical image of positive-tone photoresist nanopatterns, which were produced by using two-sided light leaking photomasks. (B) AFM height profile of the blue line across the photoresist nanopatterns in (A), suggesting that the recessed positive photoresist trenches had the depth of 70 nm. (C) SEM image of 100 nm wide Cr lines produced via the lift-off process after near-field photolithography in this approach. (D) 3D AFM topographical image of raised positive-tone photoresist nanopatterns produced via PSP. (E) Height profile of the blue line across the photoresist nanopatterns in (D) depicted that the raised positive photoresist nanopatterns had the height of 30 nm. (F) SEM image of nanoscale gap fabricated on Cr thin film via the lift-off process in PSP.

photoresist surface by using electron-beam evaporation, followed by overnight immersion of the samples in Remove PG (MicroChem Inc., USA). Finally, the samples were put in Remove PG and acetone under sonication for 5 min in turn to lift off the photoresist, allowing us to visualize the metal nanopattterns by AFM (Park Systems Co.), optical microscope (Olympus), and SEM (JEOL JSM-7600).

■ RESULTS AND DISCUSSION

It was found that the corners of PDMS reliefs replicated from silicon molds were round and the base size of the relief structure was larger than the apex size (Figure 2A–F). Both SEM cross-sectional and top-down images showed that the hard PDMS reliefs had the transitional slope size of 200 nm at the sidewalls (Figure 2A,D). The soft PDMS relief sidewalls had a little larger slope size of 250 nm because of its smaller Young modulus of soft PDMS Sylgard 184 than hard PDMS (Figure 2B).[45] When the PDMS reliefs (2 μm in height) were placed exactly over the metal source during electron-beam evaporation of a thin layer of gold (60 nm in thickness), the slopes were coated with thinner metal layer as compared with other regions or even avoided coating with metals because of the shadow effect of sidewalls (Figure 2A). Consequently, 200 nm wide two-sided apertures formed at both sides of PDMS sidewalls (Figure 2D–F and Figures S1 and S2 in the Supporting Information). By placing the obtained elastomeric photomasks into intimate contact with underlying photoresist coated surfaces and illuminating UV light through the elastomeric photomasks for photolithography, the incident light leaked from the nanoscopic apertures at the sidewalls can expose underlying photoresist. Consequently, sub-200 nm wide two-line nanopatterns with various shapes, such as straight lines, miniaturized letters, and squares, could be generated (Figure 2G–I and Figure S2 in Supporting Information). The produced Cr lines with a line width as small as 100 nm covered the areas as large as 2 × 1.5 cm^2 with 15% feature size variation (Figure 2G). The subwavelength nanopattern generation capability of this approach could be attributed to the following two reasons. On one hand, the intimate contact between the subwavelength apertures at the edges of PDMS reliefs and underlying photoresist surface produces near-field optical effect.[17,45] On the other hand, being different from the direct light exposure through the apertures vertically in conventional photolithography,[8,9,37,42] the indirect light leaked from the apertures at the slightly oblique sidewalls may shrink the feature size. We have checked the defects of 100 nm wide positive photoresist nanopatterns covering the areas of 2 × 1.5 cm^2 in Figure 2G, it was found that there were three defects across these areas. After checking the elastomeric photomask that used for generating these nanopatterns, we found that there were three similar defects at the corresponding positions of the elastomeric photomask. It confirmed that the defects on produced photoresist nanopatterns were attributed to the defects on PDMS structures of elastomeric photomask. In future work, the defects can be eliminated by optimizing the elastomeric photomask fabrication process. Besides, we also checked the feature size uniformity of the 100 nm wide positive photoresist nanopatterns covering the areas of 2 × 1.5 cm^2. It was found that the average 100 nm wide line patterns had a line width variation of 12%.

By comparing to PSP, it was found that the lithographic strategy developed here generated recessed positive photoresist trenches (Figure 3A,B), while PSP produced raised positive photoresist nanopatterns (Figure 3D,E). This is due to the opaque metal layer coating on PDMS reliefs used here blocked the transmission of all incident light except that from the sidewalls. On the contrary, the transparent PDMS reliefs used in PSP allowed for the exposure of all photoresist except that below the sidewalls. The transmitted light intensity at the sidewalls was the highest in this method, while that was the lowest in PSP. The lift-off process was utilized to generate metallic features in the standard application of photolithography. Herein, in a typical lift off process after the production of positive photoresist nanopatterns, subwavelength raised metal lines were generated in this lithographic strategy (Figure 3C), while nanoscale gaps on metal thin film were generated in PSP (Figure 3F). In order to produce raised metal

DOI: 10.1021/acs.langmuir.5b00568
Langmuir 2015, 31, 5005–5013

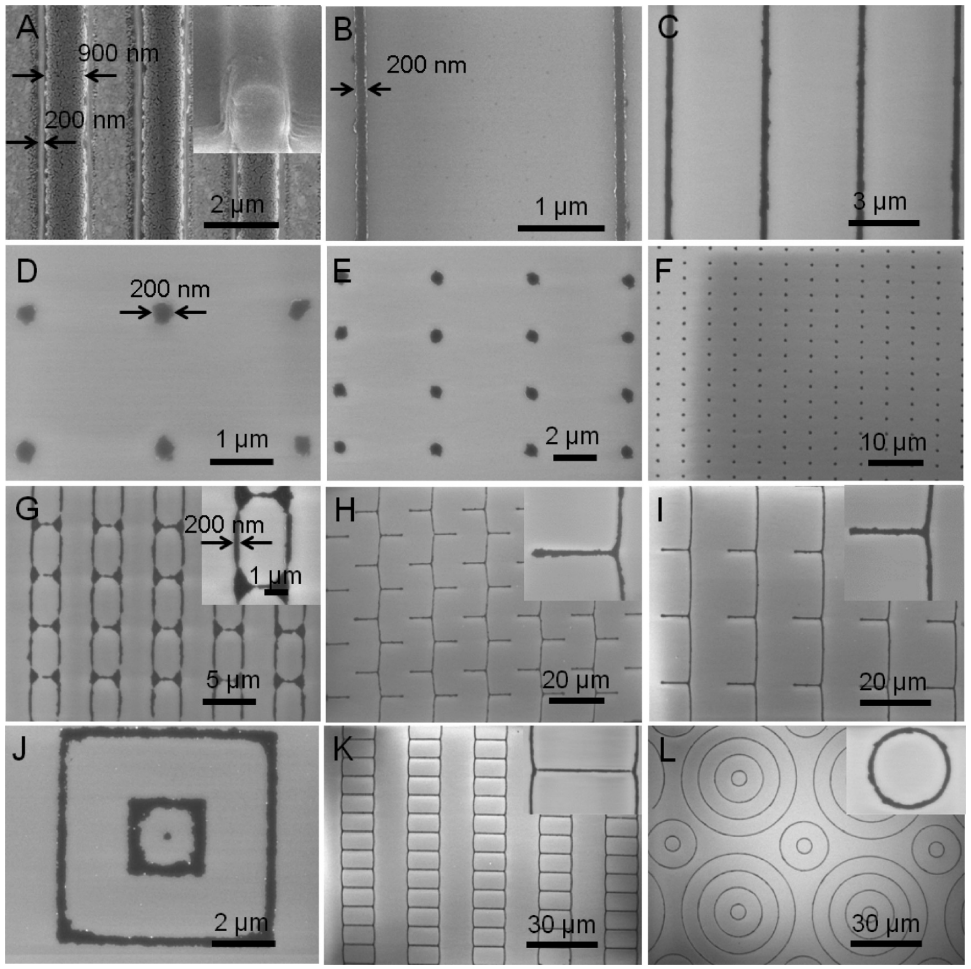

Figure 4. Fabrication of nanopatterns with uniform periodicity by using two-sided light leaking photomasks with large exposure dose and small aperture spacing. (A) SEM top-down image of two-sided light leaking photomasks with 200 nm wide apertures and 900 nm wide spacing between two nearby apertures. Inset: SEM cross-sectional image of PDMS relief. (B, C) SEM images of 200 nm wide Cr lines with the pitches of 3 and 4 μm, respectively, fabricated in this approach. (D, E, F) SEM images of 200 nm Cr dot array with the pitches of 3, 4, and 5 μm, respectively. (G) and (H–I) SEM images of Cr nanopatterns with the feature shapes of ladder and branch, respectively. (J, K, L) SEM images of Cr nanopatterns with the feature shapes of multiple-square, ladder, and multiple-circle, respectively.

line nanopatterns in PSP, wet etching was required, in which the metal residues left on the substrate and the etching time was difficult to control.[17] If the periodicity of two adjacent lines produced by the same PDMS reliefs and the periodicity of the line sets are defined as d1 and d2, respectively, d1 and d2 are determined by the size and periodicity of PDMS reliefs, respectively (Figure 3C). Hence, by changing these two parameters, the periodicities of obtained nanopatterns (both d1 and d2) could be adjusted conveniently. For example, d1 and d2 in Figure 2G were 1.1 and 3 μm, respectively, while d1 and d2 in Figure 3C were 900 nm and 3 μm, respectively. Noticeably, the subwavelength nanopatterns not only could be fabricated on positive tone photoresist surface but also could be produced on negative tone photoresist surface (Figure S3M–O in Supporting Information), indicating the flexibility and applicability of this method.

It was worth noticing that the light leaked from adjacent two-sided apertures on the same PDMS relief stripes would expose all the underlying photoresist if large exposure dose (250 mW/cm^2) and the PDMS reliefs with small apertures spacing (width d1 < 1 μm) were employed (Figure 4). In this case, the exposure from two nearby apertures would overlap with each other, leading to the merging of two close-spaced recessed photoresist trenches into one photoresist trench. Consequently, the PDMS reliefs with oblique sidewalls and round corners acted as the lens to focus the incident light below the relief structures, producing one-line nanopatterns with uniform periodicity, rather than two-line nanopatterns. Variously shaped features can be fabricated with the line width or spot size of 200 nm in this manner (Figure 4B–L).

If the substrates were not placed exactly above the metal source during e-beam evaporation process, one-sided nanoscopic apertures with the width as small as 80 nm could be generated below the sidewalls (Figure 5A–F and Figures S1B and S5 in Supporting Information) because the sidewall of each relief stripe that was further away from the metal source was blocked by the PDMS micro/nanostructures during the metal oblique evaporation. By using these PDMS reliefs with 80 nm wide one-sided apertures as the photomasks in near-field photolithography, the incident light was strictly allowed to pass from the one-sided apertures to expose underlying photoresist, producing 80 nm wide line patterns with uniform periodicity (Figure 5 and Figure S6 in Supporting Information). Since the subwavelength apertures with various shapes, such as straight lines, circle, crescent, square, rod, and L-shape, could be produced, the correspondingly shaped metal nanopatterns with

DOI: 10.1021/acs.langmuir.5b00568
Langmuir 2015, 31, 5005–5013

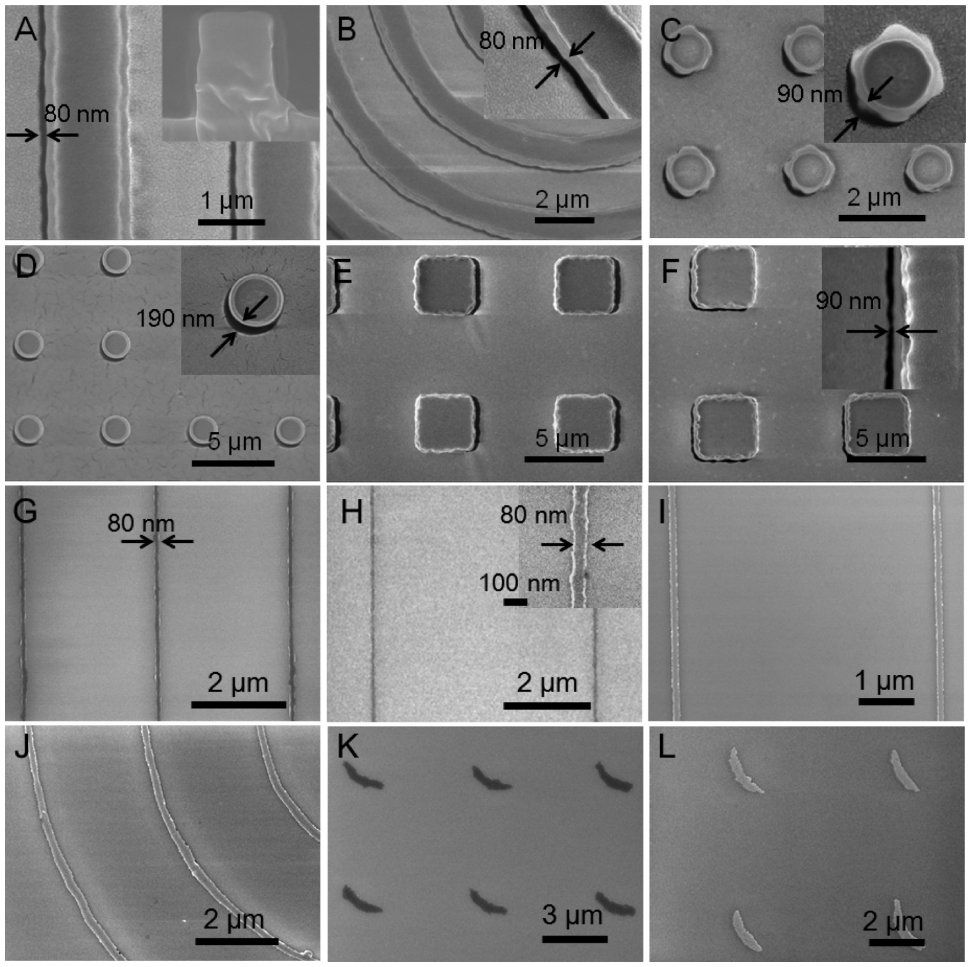

Figure 5. Fabrication of subwavelength nanopatterns with uniform periodicity by utilizing the PDMS photomasks with one-sided apertures. (A, B) SEM images of 80 nm wide apertures created at one-sided sidewalls of PDMS reliefs with the shapes of straight stripe and concentric-circle, respectively. The inset of (A) is the corresponding SEM cross-sectional image of PDMS relief. (C, D) SEM images of crescent apertures with the widths of 90 and 190 nm, respectively, created at the sidewalls of PDMS post-relief structures. (E, F) SEM images of 90 nm wide rod-shape and L-shape apertures, respectively, created at the sidewalls of PDMS square reliefs. (G, H) SEM images of 80 nm wide Cr lines with the periodicities of 3 and 5 μm, respectively. (I, J) SEM images of 150 nm wide straight and circular gold lines, respectively. (K, L) SEM images of crescent Cr and Au nanopatterns, respectively.

subwavelength line width could be produced effectively with uniform periodicity (Figure 5G−L and Figure S6 in Supporting Information). Especially, if the PDMS post relief array with nanoscopic crescent apertures created at the circular sidewalls was utilized as photomasks, crescent metal nanopatterns could be produced (Figure 5C,D,K,L), which was difficult for the conventional methods. By adjusting the position of PDMS posts during the metal evaporation process, both the dimensions and the orientation of the crescent apertures could also be programmed (Figure 5C,D and Figure S5C,D in Supporting Information). The further the PDMS structures were placed away from the metal source, the smaller the one-sided apertures were produced. Thereby the dimensions of produced metal crescent nanostructures could be tuned correspondingly (Figure 5K,L and Figure S5J−L in Supporting Information). Importantly, oblique metal evaporation not only could be utilized to produce one-sided apertures on flat PDMS reliefs but also could be employed to generate one-sided apertures on the sidewalls of V-shape PDMS reliefs (Figure S5H,I in Supporting Information).

In addition to the metal evaporation direction, the height of PDMS reliefs can also dictate the aperture geometries and shapes. In this work, nanoscopic apertures were created on the sidewalls of PDMS reliefs with the height ranging from 500 nm to 2 μm (Figure S7 in Supporting Information). The aperture widths ranging from 80 to 200 nm were generated at the sidewalls of PDMS reliefs in this work. If the height of PDMS reliefs was decreased to 260 nm, the 60 nm thick gold layer covered the whole sidewalls, and no apertures formed. Noticing that evident variation in aperture size and the produced feature size were not found after repeated usage of the photomask for 30 times, it demonstrated the good reusability of this kind of photomask (Figure S8 in Supporting Information).

To prove that the incident light can transmit from the relatively thin metal coated oblique sidewalls to expose underlying photoresist below the sidewalls selectively, we designed the PDMS reliefs with adjustable size of oblique sidewalls intentionally (Figure 6A−C). We hypothesize that the effective exposure dose below the oblique sidewalls should be larger than that below the flat areas for both the naturally formed oblique sidewalls and intentionally designed oblique sidewalls. This was because that the thick opaque metal layer at the flat parts could block the incident light more effectively than the thin metal layer did at the oblique sidewalls. By using KOH

DOI: 10.1021/acs.langmuir.5b00568
Langmuir 2015, 31, 5005−5013

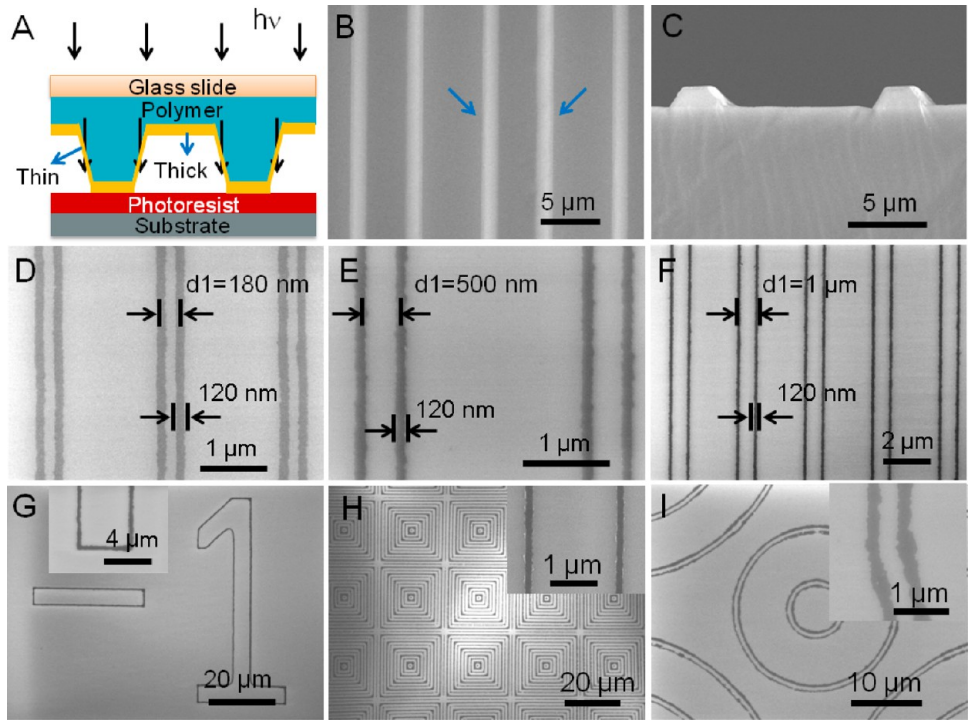

Figure 6. Subwavelength photolithography using metal-coated PDMS photomasks with intentionally designed oblique sidewalls without apertures. (A) Schematic illustrating that light leaks from thin metal coated large oblique sidewalls of PDMS reliefs to expose underlying photoresist, producing two-line subwavelength nanopatterns. (B) SEM top-down image of the PDMS light leaking photomask with the shape of straight stripe, on which the gold coating at the oblique sidewalls was thinner than that at the flat areas. The blue arrow indicated white regions were the two-sided oblique sidewalls. (C) SEM cross-sectional image showing the profile of PDMS reliefs with oblique sidewalls. (D–F) SEM images of 120 nm wide Cr two-line patterns with varying periodicities fabricated by utilizing the light leaking photomasks with thin metal-coated sidewalls: (D) d1 spacing: 180 nm, d2 spacing: 2 μm; (E) d1 spacing: 500 nm, d2 spacing: 3 μm; (F) d1 spacing: 1 μm, d2 spacing: 3 μm. (G) SEM image of Cr nanopatterns with the shape of miniaturized letters of "-1". (H, I) SEM images of Cr nanopatterns with the shapes of multiple-square and multiple-circle, respectively.

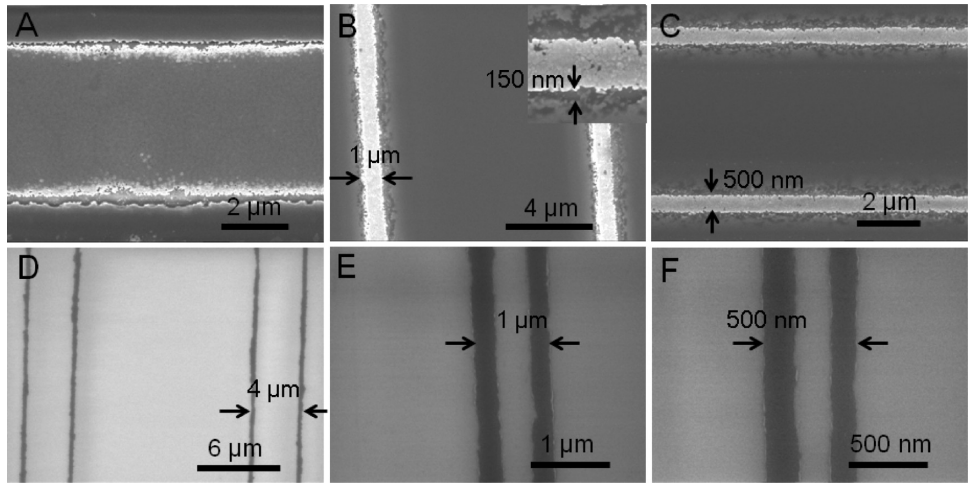

Figure 7. Near-field photolithography using the photomasks with nanoscopic apertures created at the size-adjustable oblique sidewalls. (A, B, C) SEM images of metal-coated PDMS relief photomasks with 150 nm wide apertures created at the two sides of PDMS relief apexes with the aperture spacing of 4 μm, 1 μm, and 500 nm, respectively. (D, E, F) SEM images of Cr nanopatterns with the d1 spacing of 4 μm, 1 μm, and 500 nm, respectively, which were fabricated by utilizing the photomasks in (A, B, C), respectively.

anisotropic etching with controlled etching time, silicon reliefs with oblique sidewalls could be obtained with adjustable sidewall size (Figure S9 in Supporting Information). Consequently, corresponding PDMS reliefs with adjustable oblique sidewalls could be replicated from the silicon molds with the angle θ of 54.7° (Figure S10 in Supporting Information). By employing vertical evaporation of metals toward the PDMS reliefs with oblique sidewalls, the metal layer at the oblique sidewalls was thinner than that at the flat places (Figure 6A). This phenomenon could not only be calculated theoretically (Supporting text and Figure S11 in Supporting Information) but also could be substantiated via experiment (Figure S12 in Supporting Information). By calculation, it was found that the thickness of metal layer at the oblique sidewalls was only one-

DOI: 10.1021/acs.langmuir.5b00568
Langmuir 2015, 31, 5005–5013

third of that at the flat areas (Supporting text). For example, 60 nm thick gold coating layer was obtained at the flat areas in this work, and therefore 20 nm thick gold coating layer was achieved at the oblique sidewalls. By using such photomasks, the photoresist underlying the oblique sidewalls could be selectively exposed completely by utilizing appropriate exposure dose (250 mW/cm^2). As a result, variously shaped two-line nanopatterns with the line width as small as 120 nm and adjustable periodicities could be obtained (Figure 6D–I). Significantly, the smallest periodicity of 180 nm between adjacent Cr lines could be achieved in this approach (Figure 6D). By putting the obtained gold-coated photomasks in gold etching solution with designated etching time, it was found that the gold layer at the sidewalls disappeared faster than that at other regions, indicating that the gold layer at the sidewalls was thinner than that at the flat regions (Figure S12 in Supporting Information).

Nanoscopic apertures could also be formed at the oblique sidewalls of reliefs via selective wet etching of the metal at the sidewalls with poly(methyl methacrylate) PMMA as the protective layer at other places (Figures 1C and 7 and Figure S13 in Supporting Information). By utilizing the obtained photomasks in near-field photolithography, the incident light could be strictly allowed to pass through the nanoscopic apertures, leading to formation of two-line subwavelength photoresist nanopatterns (Figure 7). Compared to the aforementioned apertures created at the sidewalls by line-of-sight metal evaporation in one step, the distinctive advantage of the PDMS photomasks with nanoscopic apertures created at the oblique sidewalls by etching is the capability to tailor the spacing of produced nanopatterns without the requirement of designing new photomasks. By utilizing different KOH etching time in producing the silicon master, the apex size of silicon trenches could be adjusted conveniently (Figure S9 in Supporting Information). Since the nanoscopic apertures were constructed at two sides of the apexes on the Au-coated PDMS reliefs and the apex size defined the periodicity of produced nanopatterns, the aperture spacing on PDMS reliefs could be well controlled (Figure 7A–C). As such, the metal nanopatterns with adjustable d1 spacing could be achieved by utilizing the original photomask with a fixed feature size of 2 μm (Figure 7E,F).

SUMMARY AND CONCLUSIONS

In summary, a low-cost and effective near-field photolithography strategy was developed to enable the formation of sub-100 nm variously shaped nanopatterns over centimeter-scale areas. The key in this study is the discovery of narrow transitional oblique sidewalls at the PDMS reliefs, on which nanoscopic apertures formed by coating an opaque metal layer. By using this novel photomask to modulate the transmission light intensity at the sidewalls at nanoscale regions, subwavelength nanopatterns were fabricated with controllable size, shape, and periodicity. More importantly, the photomasks were fabricated via a facile one-step method with the aid of line-of-sight electron-beam evaporation, bypassing extra steps of creating apertures after metal coating. This near-field photolithography strategy could be a good alternative to PSP and BPL, since it produced recessed positive photoresist nanopatterns while PSP produced raised positive photoresist nanopatterns. Since the PDMS photomasks used here can be fabricated on wafer-scale quartz surfaces, it is possible to use wafer-scale light leaking photomasks fitted in the mask aligner to produce wafer-scale subwavelength nanopatterns as well. Coupled with photochemistry, this lithographic strategy is possible to be utilized in fabrication of nanoscale chemical patterns as well.[37,41] The fabricated large-area metal nanopatterns are suitable to be used in various applications, such as studying the cell matrix interaction and stem cell differentiation behaviors.[12−14,48]

ASSOCIATED CONTENT

Supporting Information

Calculation of the relationship between the thickness of metal layer at the oblique sidewalls and that at the flat areas, schematic illustrating the dependence of the formation of two-sided apertures and one-sided apertures on the metal evaporation directions, creation of nanoscopic apertures at the oblique sidewalls of metal-coated PDMS relief structures, SEM images and AFM images of PDMS photomasks with two-sided apertures, one-sided apertures and corresponding produced nanopatterns, investigation on the reusability of elastomeric photomasks, SEM images of silicon molds and corresponding PDMS photomasks with intentionally designed size-controllable sidewalls. This material is available free of charge via the Internet at http://pubs.acs.org.

AUTHOR INFORMATION

Corresponding Author

*E-mail FWHUO@ntu.edu.sg (F.H.).

Notes

The authors declare no competing financial interest.

ACKNOWLEDGMENTS

F.H. acknowledges the financial support from the AcRF Tier 2 (RG 17/12) from the Ministry of Education, Singapore.

REFERENCES

(1) Wagner, C.; Harned, N. EUV lithography: Lithography gets extreme. *Nat. Photonics* **2010**, *4*, 24−26.

(2) Liu, G. L.; Eichelsdoerfer, D. J.; Rasin, B.; Zhou, Y.; Brown, K. A.; Liao, X.; Mirkin, C. A. Delineating the pathways for the site-directed synthesis of individual nanoparticles on surfaces. *Proc. Natl. Acad. Sci. U. S. A.* **2013**, *110*, 887−891.

(3) Wu, J.; Yu, C. H.; Li, S. Z.; Zou, B. H.; Liu, Y. Y.; Zhu, X. Q.; Guo, Y. Y.; Xu, H. B.; Zhang, W. N.; Zhang, L. P.; Liu, B.; Tian, D. B.; Huang, W.; Sheetz, M. P.; Huo, F. W. Parallel near-field photolithography with metal-coated elastomeric masks. *Langmuir* **2015**, *31*, 1210−1217.

(4) Wu, J.; Zan, X. L.; Li, S. Z.; Liu, Y. Y.; Cui, C. L.; Zou, B. H.; Zhang, W. N.; Xu, H. B.; Duan, H. W.; Tian, D. B.; Huang, W.; Huo, F. W. In situ synthesis of large-area single sub-10 nm nanoparticle arrays by polymer pen lithography. *Nanoscale* **2014**, *6*, 749−752.

(5) Martin-Fabiani, I.; Riedel, S.; Rueda, D. R.; Siegel, J.; Boneberg, J.; Ezquerra, T. A.; Nogales, A. Micro- and submicrostructuring thin polymer films with two and three-beam single pulse laser interference lithography. *Langmuir* **2014**, *30*, 8973−8979.

(6) Meng, X. H.; Zhang, X. P.; Ye, L.; Qiu, D. Fabrication of large-sized two-dimensional ordered surface array with well-controlled structure via colloidal particle lithography. *Langmuir* **2014**, *30*, 7024−7029.

(7) Lee, S. K.; Jung, J. M.; Lee, J. S.; Jung, H. T. Fabrication of complex patterns with a wide range of feature sizes from a single line prepattern by successive application of capillary force lithography. *Langmuir* **2010**, *26*, 14359−14363.

(8) Liao, X.; Brown, K. A.; Schmucker, A. L.; Liu, G.; He, S.; Shim, W.; Mirkin, C. A. Desktop nanofabrication with massively multiplexed beam pen lithography. *Nat. Commun.* **2013**, *4*, 2103.

DOI: 10.1021/acs.langmuir.5b00568
Langmuir 2015, 31, 5005−5013

(9) Huo, F. W.; Zheng, G. F.; Liao, X.; Giam, L. R.; Chai, J. A.; Chen, X. D.; Shim, W. Y.; Mirkin, C. A. Beam pen lithography. *Nat. Nanotechnol.* **2010**, *5*, 637−640.
(10) Yao, X.; Peng, R.; Ding, J. D. Cell-material interactions revealed via material techniques of surface patterning. *Adv. Mater.* **2013**, *25*, 5257−5286.
(11) Giam, L. R.; Massich, M. D.; Hao, L. L.; Wong, L. S.; Mader, C. C.; Mirkin, C. A. Scanning probe-enabled nanocombinatorics define the relationship between fibronectin feature size and stem cell fate. *Proc. Natl. Acad. Sci. U. S. A.* **2012**, *109*, 4377−4382.
(12) Salaita, K.; Nair, P. M.; Petit, R. S.; Neve, R. M.; Das, D.; Gray, J. W.; Groves, J. T. Restriction of receptor movement alters cellular response: physical force sensing by EphA2. *Science* **2010**, *327*, 1380−1385.
(13) Yu, C. h.; Law, J. B. K.; Suryana, M.; Low, H. Y.; Sheetz, M. P. Early integrin binding to Arg-Gly-Asp peptide activates actin polymerization and contractile movement that stimulates outward translocation. *Proc. Natl. Acad. Sci. U. S. A.* **2011**, *108*, 20585−20590.
(14) Nair, P. M.; Salaita, K.; Petit, R. S.; Groves, J. T. Using patterned supported lipid membranes to investigate the role of receptor organization in intercellular signaling. *Nat. Protoc.* **2011**, *6*, 523−539.
(15) Bowen, A. M.; Motala, M. J.; Lucas, J. M.; Gupta, S.; Baca, A. J.; Mihi, A.; Alivisatos, A. P.; Braun, P. V.; Nuzzo, R. G. Triangular elastomeric stamps for optical applications: Near-field phase shift photolithography, 3D proximity field patterning, embossed antireflective coatings, and SERS sensing. *Adv. Funct. Mater.* **2012**, *22*, 2927−2938.
(16) Rogers, J. A.; Paul, K. E.; Jackman, R. J.; Whitesides, G. M. Using an elastomeric phase mask for sub-100 nm photolithography in the optical near field. *Appl. Phys. Lett.* **1997**, *70*, 2658−2660.
(17) Lee, T. W.; Jeon, S.; Maria, J.; Zaumseil, J.; Hsu, J. W. P.; Rogers, J. A. Soft-contact optical lithography using transparent elastomeric stamps: application to nanopatterned organic light-emitting devices. *Adv. Funct. Mater.* **2005**, *15*, 1435−1439.
(18) del Campo, A.; Arzt, E. Fabrication approaches for generating complex micro- and nanopatterns on polymeric surfaces. *Chem. Rev.* **2008**, *108*, 911−945.
(19) Zhou, Y.; Xie, Z.; Brown, K. A.; Park, D. J.; Zhou, X.; Chen, P. C.; Hirtz, M.; Lin, Q. Y.; Dravid, V. P.; Schatz, G. C.; Zheng, Z.; Mirkin, C. A. Apertureless cantilever-free pen arrays for scanning photochemical printing. *Small* **2014**, *11*, 913−918.
(20) Qin, D.; Xia, Y. N.; Whitesides, G. M. Soft lithography for micro- and nanoscale patterning. *Nat. Protoc.* **2010**, *5*, 491−502.
(21) Braunschweig, A. B.; Huo, F. W.; Mirkin, C. A. Molecular printing. *Nat. Chem.* **2009**, *1*, 353−358.
(22) Henzie, J.; Lee, J.; Lee, M. H.; Hasan, W.; Odom, T. W. Nanofabrication of Plasmonic Structures*. *Annu. Rev. Phys. Chem.* **2009**, *60*, 147−165.
(23) Choi, J.; Lee, K.; Janes, D. B. Nanometer scale gap made by conventional microscale fabrication: Step junction. *Nano Lett.* **2004**, *4*, 1699−1703.
(24) Sun, L. F.; Chin, S. N.; Marx, E.; Curtis, K. S.; Greenham, N. C.; Ford, C. J. B. Shadow- evaporated nanometre-sized gaps and their use in electrical studies of nanocrystals. *Nanotechnology* **2005**, *16*, 631−634.
(25) Laza, S. C.; Polo, M.; Neves, A. A.; Cingolani, R.; Camposeo, A.; Pisignano, D. Two-photon continuous flow lithography. *Adv. Mater.* **2012**, *24*, 1304−1308.
(26) Ok, J. G.; Kwak, M. K.; Huard, C. M.; Youn, H. S.; Guo, L. J. Photo-roll lithography (PRL) for continuous and scalable patterning with application in flexible electronics. *Adv. Mater.* **2013**, *25*, 6554−6561.
(27) Craighead, H. G. 10-nm line width electron beam lithography on GaAs. *Appl. Phys. Lett.* **1983**, *42*, 38−40.
(28) Kim, J.; Shin, Y. H.; Yun, S. H.; Choi, D. S.; Nam, J. H.; Kim, S. R.; Moon, S. K.; Chung, B. H.; Lee, J. H.; Kim, J. H.; Kim, K. Y.; Kim, K. M.; Lim, J. H. Direct-write patterning of bacterial cells by dip-pen nanolithography. *J. Am. Chem. Soc.* **2012**, *134*, 16500−16503.
(29) Zhang, X.; Weeks, B. L. Tip induced crystallization lithography. *J. Am. Chem. Soc.* **2014**, *136*, 1253−1255.
(30) Chai, J. A.; Huo, F. W.; Zheng, Z. J.; Giam, L. R.; Shim, W.; Mirkin, C. A. Scanning probe block copolymer lithography. *Proc. Natl. Acad. Sci. U. S. A.* **2010**, *107*, 20202−20206.
(31) Ruiz, R.; Kang, H.; Detcheverry, F. A.; Dobisz, E.; Kercher, D. S.; Albrecht, T. R.; de Pablo, J. J.; Nealey, P. F. Density multiplication and improved lithography by directed block copolymer assembly. *Science* **2008**, *321*, 936−939.
(32) Divliansky, I.; Mayer, T. S.; Holliday, K. S.; Crespi, V. H. Fabrication of three-dimensional polymer photonic crystal structures using single diffraction element interference lithography. *Appl. Phys. Lett.* **2003**, *82*, 1667−1669.
(33) Huo, F. W.; Zheng, Z. J.; Zheng, G. F.; Giam, L. R.; Zhang, H.; Mirkin, C. A. Polymer pen lithography. *Science* **2008**, *321*, 1658−1660.
(34) Kurland, N. E.; Dey, T.; Wang, C.; Kundu, S. C.; Yadavalli, V. K. Silk protein lithography as a route to fabricate sericin microarchitectures. *Adv. Mater.* **2014**, *26*, 4431−4437.
(35) Henzie, J.; Lee, M. H.; Odom, T. W. Multiscale patterning of plasmonic metamaterials. *Nat. Nanotechnol.* **2007**, *2*, 549−554.
(36) Srituravanich, W.; Pan, L.; Wang, Y.; Sun, C.; Bogy, D. B.; Zhang, X. Flying plasmonic lens in the near field for high-speed nanolithography. *Nat. Nanotechnol.* **2008**, *3*, 733−737.
(37) Leggett, G. J. Light-directed nanosynthesis: near-field optical approaches to integration of the top-down and bottom-up fabrication paradigms. *Nanoscale* **2012**, *4*, 1840−1855.
(38) Stender, C. L.; Greyson, E. C.; Babayan, Y.; Odom, T. W. Patterned MoS_2 nanostructures over centimeter-square areas. *Adv. Mater.* **2005**, *17*, 2837−2841.
(39) ul Haq, E.; Liu, Z.; Zhang, Y.; Ahmad, S. A.; Wong, L. S.; Armes, S. P.; Hobbs, J. K.; Leggett, G. J.; Micklefield, J.; Roberts, C. J.; Weaver, J. M. Parallel scanning near-field photolithography: the snomipede. *Nano Lett.* **2010**, *10*, 4375−4380.
(40) Qin, D.; Xia, Y. N.; Black, A. J.; Whitesides, G. M. Photolithography with transparent reflective photomasks. *J. Vac. Sci. Technol., B* **1998**, *16*, 98−103.
(41) Bian, S.; Zieba, S. B.; Morris, W.; Han, X.; Richter, D. C.; Brown, K. A.; Mirkin, C. A.; Braunschweig, A. B. Beam pen lithography as a new tool for spatially controlled photochemistry, and its utilization in the synthesis of multivalent glycan arrays. *Chem. Sci.* **2014**, *5*, 2023−2030.
(42) Kim, S.; Jung, H.; Kim, Y.; Jang, J.; Hahn, J. W. Resolution limit in plasmonic lithography for practical applications beyond 2x-nm half pitch. *Adv. Mater.* **2012**, *24*, OP337−OP344.
(43) Rogers, J. A.; Paul, K. E.; Jackman, R. J.; Whitesides, G. M. Generating ∼90 nm features using near-field contact-mode photolithography with an elastomeric phase mask. *J. Vac. Sci. Technol., B* **1998**, *16*, 59−68.
(44) Gates, B. D.; Xu, Q.; Love, J. C.; Wolfe, D. B.; Whitesides, G. M. Unconventional nanofabrication. *Annu. Rev. Mater. Res.* **2004**, *34*, 339−372.
(45) Odom, T. W.; Love, J. C.; Wolfe, D. B.; Paul, K. E.; Whitesides, G. M. Improved pattern transfer in soft lithography using composite stamps. *Langmuir* **2002**, *18*, 5314−5320.
(46) Solak, H. H.; David, C.; Gobrecht, J.; Golovkina, V.; Cerrina, F.; Kim, S. O.; Nealey, P. F. Sub-50 nm period patterns with EUV interference lithography. *Microelectron. Eng.* **2003**, *67*−*68*, 56−62.
(47) Lee, S. W.; Lee, S. S. Shrinkage ratio of PDMS and its alignment method for the wafer level process. *Microsyst. Technol.* **2007**, *14*, 205−208.
(48) Yu, C. H.; Groves, J. T. Engineering supported membranes for cell biology. *Med. Biol. Eng. Comput.* **2010**, *48*, 955−963.

DOI: 10.1021/acs.langmuir.5b00568
Langmuir 2015, 31, 5005−5013